Diamond-Shaped Heterometallic Complexes of Iron(II) and Copper(I) Bridged by Cyanide Groups Containing Monodentate or Bidentate Phosphanes Bound to Copper(I), Including an Alternative Structure Based on the Nature of the Bidentate Phosphane Ligand

Donald J. Darensbourg,*[a] Way-Zen Lee,[a] M. Jason Adams,[a] and Jason C. Yarbrough[a]

Keywords: Copper / Iron / P ligands / Cyanides / Bridging ligands

The diamond-shaped heterometallic cyanide-bridged complex of iron(II) and copper(I), $[CpFe(CO)(\mu\text{-}CN)_2Cu(CH_3CN)_2]_2$ (**1**), has been synthesized from the reaction of $K[CpFe(CO)(CN)_2]$ and $[Cu(CH_3CN)_4][BF_4]$ in acetonitrile. Upon the addition of 2–4 equivalents of phosphane ligands to complex **1**, the coordination geometry of the copper centers can be varied from trigonal planar as in $[CpFe(CO)(\mu\text{-}CN)_2Cu(PCy_3)]_2$ (**2**), to tetrahedral as found in $[CpFe(CO)(\mu\text{-}CN)_2Cu(PCy_3)_2]_2$ (**3**). Analogous derivatives containing other phosphane ligands, namely PMe_3, P(*p*-tolyl)$_3$, PMe_2Ph, and PPh_2Me have been synthesized as well. Prolonged exposure of complex **3** in CH_2Cl_2 to excess PCy_3 has provided the bimetallic complex $[CpFe(PCy_3)(CN)(\mu\text{-}CN)Cu(PCy_3)_2]$ (**4**), where the metal aggregate is disrupted and PCy_3 has displaced CO at the iron center. Bidentate phosphane analogs of complex **3** have been prepared by adding two equivalents of dcpe [bis(dicyclohexylphosphanyl)-ethane] or dcpp [bis(dicyclohexylphosphanyl)propane] to complex **1**. The solid-state structures of several of these diamond-shaped derivatives, in addition to complex **4**, have been determined by X-ray crystallography. The overlapping diamond-shaped $[Fe_2(CN)_4Cu_2]$ cores, which form channels within the solids, are blocked by bulky, copper-bound phosphane ligands such as PCy_3. However, in the case of the small phosphane PMe_3, or the chelating phosphanes dcpe and dcpp, these channels are not blocked by the phosphane ligands; solvent molecules occupy the channels created by the overlapping metal cores instead. Alternatively, the complex $[CpFe(CO)(CN)(\mu\text{-}CN)Cu(dcpm)]_2$ (**13**), derived from bis(dicyclohexylphosphanyl)methane(dcpm), possesses two copper(I) centers, each in a distorted trigonal coordination geometry, bridged by two dcpm ligands to form an eight-membered metallacycle with a short $Cu^I\cdots Cu^I$ separation of 2.844 Å. The third ligand completing each copper's coordination sphere is a nitrogen-bound bridging cyanide group from a $CpFe(CO)(CN)_2^-$ anion.

Introduction

The use of linkage groups for assembling multinuclear complexes has been extensively investigated. A variety of polygons of transition metal complexes has been created using different linkage groups.[1] Among these, molecular squares are the most common of the metallacyclic polygons which have been prepared and structurally characterized. Included in these are one-, two-, and three-dimensional complexes which have been synthesized employing bridging cyanide groups of $M_x(CN)_y$ building blocks.[2–25] Recently, the research groups of Rauchfuss,[26] and Long[27] have reported remarkable molecular boxes, cages, and clusters made from $M(CN)_3$ or $M_6Q_6(CN)_6$ (Q = S, Se, or Te) building blocks. Other studies ranging from the electronic communication between metal atoms, i.e. electron transfer, mixed-valence, and magnetic interactions,[28] to the understanding of cyanide's role as a respiratory inhibitor in heme-copper oxidases, involve the investigation of metal cyanide complexes.[29]

Recently, we have communicated our initial investigations of the synthesis and characterization of diamond-shaped heterometallic cyanide-bridged complexes of iron(II) and copper(I) with tricyclohexylphosphane ligands coordinated to the copper(I) centers.[30] These studies showed that the coordination geometries of the copper(I) centers in the complexes $[CpFe(CO)(\mu\text{-}CN)_2Cu(PCy_3)_n]_2$ (Cp = η^5-C_5H_5; n = 1 or 2) vary from trigonal planar (n = 1) to tetrahedral (n = 2) upon the addition of a phosphane ligand. Herein we elaborate upon these investigations employing a variety of monodentate and bidentate phosphanes. Hopefully, these results will yield the necessary knowledge to allow us to expand our studies to dimeric cyanide-bridged complexes of iron(II) and zinc(II), the latter of which may serve to mimic the double metal cyanide (DMC) catalysts employed in the homopolymerization of epoxides or the copolymerization of CO_2/epoxides.[31]

Results and Discussion

Synthesis and Infrared Spectroscopy

Upon reacting $K[CpFe(CO)(CN)_2]$ (Cp = η^5-C_5H_5) with $[Cu(CH_3CN)_4][BF_4]$ in acetonitrile at ambient temperature, a clear yellow solution of $[CpFe(CO)(\mu\text{-}CN)_2Cu(CH_3CN)_2]_2$ (**1**) and a fine pale gray solid of KBF_4 were formed immediately. Two CN and one CO absorption bands in the infrared spectrum of complex **1** were observed at higher frequencies [2125 sh, 2118**s** (ν_{CN}); 1974 vs cm^{-1}

[a] Department of Chemistry, Texas A&M University, P. O. Box 30012, College Station, Texas, 77842-3012, USA

  1434–1948/01/1111–2811 $ 17.50+.50/0

Table 1. Infrared spectroscopic data in ν_{CN} and ν_{CO} regions

Compound	Condition	ν_{CN} (cm^{-1})	ν_{CO} (cm^{-1})
$K[CpFe(CO)(CN)_2]$	CH_3CN	2094 w, 2088 w	1949 vs
	KBr	2095 w, 2085 w	1973 s, 1954 s
$[CpFe(CO)(\mu\text{-}CN)_2Cu(CH_3CN)_2]_2$ (**1**)	CH_3CN	2125 sh, 2118 s	1974 vs
	CH_2Cl_2	2137 s, 2123 s	1990 vs
	KBr	2131 sh, 2118 s	1981vs
$[CpFe(CO)(\mu\text{-}CN)_2Cu(PPh_3)_{1\ or\ 2}]_2$ (**1a**)	KBr	2118 sh, 2112 s	1964 vs
$[CpFe(CO)(\mu\text{-}CN)_2Cu(PCy_3)]_2$ (**2**)	CH_2Cl_2	2115 s	1974 vs
$[CpFe(CO)(\mu\text{-}CN)_2Cu(PCy_3)_2]_2$ (**3**)	CH_3CN	2105 s, 2095 s	1959 vs
	CH_2Cl_2	2105 s, 2093 s	1963 vs
$[CpFe(PCy_3)(CN)(\mu\text{-}CN)_2Cu(PCy_3)_2]$ (**4**)	CH_2Cl_2	2062 s, 2049 s	
$[CpFe(CO)(\mu\text{-}CN)_2Cu\{P(p\text{-tolyl})_3\}]_2$ (**5**)	CH_3CN	2120 sh, 2114 s	1970 vs
	CH_2Cl_2	2127 s, 2114 s	1983 vs
$[CpFe(CO)(\mu\text{-}CN)_2Cu\{P(p\text{-tolyl})_3\}_2]_2$ (**6**)	CH_3CN	2112 s	1964 vs
	CH_2Cl_2	2121 s, 2095 sh	1970 vs
	THF	2120 s	1968 vs
$[CpFe(CO)(\mu\text{-}CN)_2Cu(PMePh_2)]_2$ (**7**)	CH_3CN	2114 s	1970 vs
$[CpFe(CO)(\mu\text{-}CN)_2Cu(PMe_2Ph)]_2$ (**8**)	CH_3CN	2115 s	1971 vs
$[CpFe(CO)(\mu\text{-}CN)_2Cu(PMe_3)]_2$ (**9**)	CH_3CN	2115s	1971 vs
	CH_2Cl_2	2119s	1977 vs
$[CpFe(CO)(\mu\text{-}CN)_2Cu(PMePh_2)_2]_2$ (**10**)	CH_3CN	2110 m, 2095 s	1958 vs
$[CpFe(CO)(\mu\text{-}CN)_2Cu(PMe_2Ph)_2]_2$ (**11**)	CH_3CN	2110 m, 2095 s	1956 vs
$[CpFe(CO)(\mu\text{-}CN)_2Cu(PMe_3)_2]_2$ (**12**)	CH_3CN	2110 m, 2095 s	1956 vs
	CH_2Cl_2	2108 s, 2092 s	1963 vs
$[CpFe(CO)(CN)(\mu\text{-}CN)Cu(dcpm)]_2$ (**13**)	CH_2Cl_2	2101, 2092	1964
$[CpFe(CO)(\mu\text{-}CN)_2Cu(dcpe)]_2$ (**14**)	CH_2Cl_2	2121, 2111	1970
$[CpFe(CO)(\mu\text{-}CN)_2Cu(dcpp)]_2$ (**15**)	CH_2Cl_2	2111, 2093	1964
$[CpFe(CO)(\mu\text{-}CN)_2Cu(dcpb)]_{2v}$ (**16**)	CH_2Cl_2	2108, 2093	1965

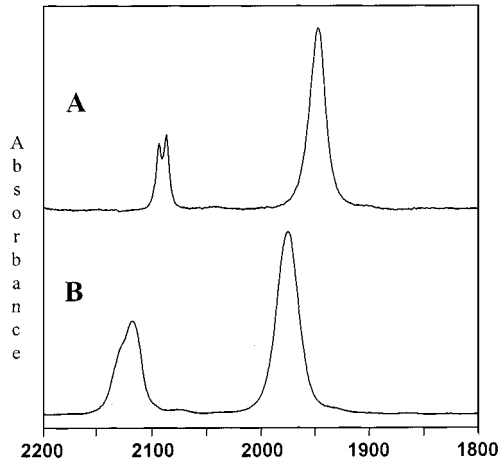

Figure 1. Infrared spectra of: **A**: [K][CpFe(CO)$(CN)_2$], and **B**: $[CpFe(CO)(\mu\text{-}CN)_2Cu(CH_3CN)_2]_2$

(ν_{CO}), Table 1] than in the parent anion $CpFe(CO)(CN)_2^-$. The absolute intensity of the ν_{CN} bands vs. that of the CO stretching vibration of **1** was increased by a factor of 2.1 times that of the corresponding bands in the parent anion (Figure 1).

The greater intensities and higher frequencies of the CN bands are evidence that the CN groups of the $CpFe(CO)(CN)_2^-$ unit are ligated to Cu^I centers in complex **1**. Two acetonitrile molecules are expected to complete each copper's coordination sphere. When the reaction was carried out in dichloromethane, free acetonitrile was observed in the infrared spectrum of the resulting solution, with the CN and CO bands being shifted to higher frequencies (Figure 2). These observations indicate that the acetonitrile molecules are dissociated from the copper(I) centers in dichloromethane solution, thereby making the metal more electron deficient. This in turn leads to a significant withdrawal of electron density from the nitrogens of the bridging cyanides to the Cu^I centers, and the frequencies of the CN and CO vibrational modes are shifted to significantly higher frequencies than those seen in complex **1**. Nevertheless, it is most likely that in this instance there are weak Cu···Cl interactions with dichloromethane. In the absence of strongly coordinating solvents, the complex was unstable under an argon atmosphere and decomposed within 3−4 h.

A turbid solution resulted immediately upon adding triphenylphosphane to an acetonitrile solution of **1**, with subsequent formation of a yellow solid after several minutes of stirring at ambient temperature. The isolated yellow solid was found to be insoluble in all common organic solvents. However, the solid-state infrared spectrum of this material (**1a**) exhibited ν_{CN} and ν_{CO} vibrational modes of lower frequencies than those observed in complex **1**, and hence indicate the binding of PPh_3 ligands at the copper(I) centers. In order to obtain an analogous complex which was soluble in organic solvent, complex **1** was reacted with tricyclohexylphosphane. In this manner, two complexes, $[CpFe(CO)(\mu\text{-}CN)_2Cu(PCy_3)]_2$ (**2**) and $[CpFe(CO)(\mu\text{-}CN)_2Cu(PCy_3)_2]_2$ (**3**), were synthesized by the reaction of **1** with two or four equivalents of PCy_3, respectively.[30] Whereas, complex **2** precipitated directly from the acetonitrile reaction solution,

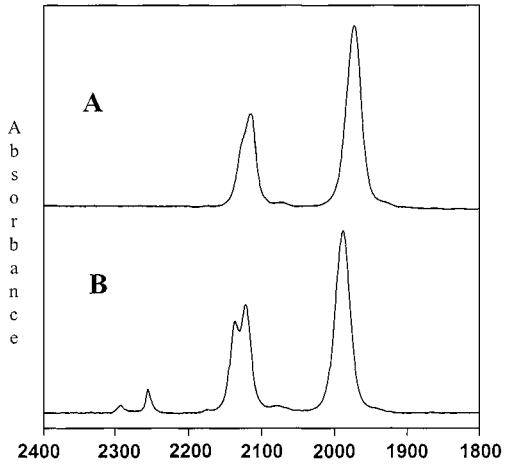

Figure 2. Infrared spectra of: **A** $[CpFe(CO)(\mu\text{-}CN)_2Cu(CH_3CN)_2]_2$, and **B**: $[CpFe(CO)(\mu\text{-}CN)_2Cu]$

complex **3** remained in solution; both derivatives were readily soluble in dichloromethane. As seen in Table 1, the ν_{CN} and ν_{CO} bands progressively shift to lower frequencies in proceeding from complex **1** to **2** and **3**, consistent with one and two equivalents of PCy_3 binding to the Cu^I centers. The subsequent addition of PCy_3 to complex **3** in dichloromethane with stirring over a period of time affords a complex devoid of any CO ligand which has been characterized as $[CpFe(PCy_3)(CN)(\mu\text{-}CN)Cu(PCy_3)_2]$ (**4**) (vide infra). Scheme 1 summarizes the sequence of reactions employed in the synthesis of **2** and **3** and other phosphane analogs, along with further reaction pathways of these derivatives.

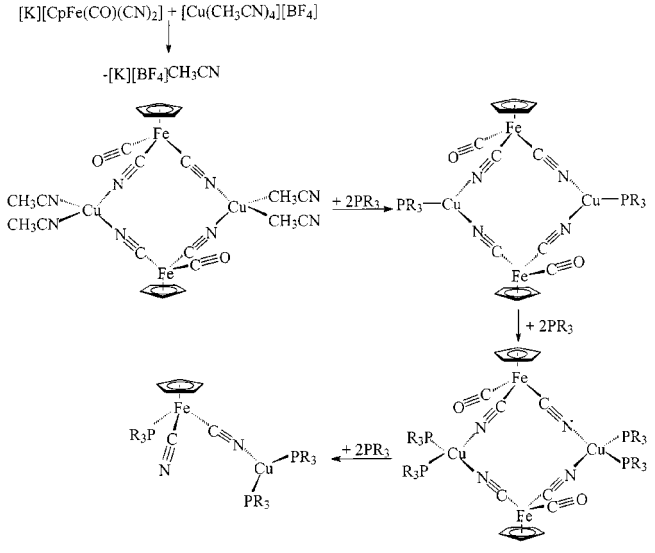

Scheme 1

In an effort to prepare soluble derivatives containing a phosphane ligand that closely mimics the electronic and steric properties of PPh_3, we synthesized the $P(p\text{-tolyl})_3$ derivatives. Upon adding two equivalents of $P(p\text{-tolyl})_3$ to complex **1** in acetonitrile, a yellow solution of $[CpFe(CO)(\mu\text{-}CN)_2Cu\{P(p\text{-tolyl})_3\}]_2$ (**5**) was obtained. Unfortunately, complex **5** was unstable in acetonitrile or dichloromethane solution, even when maintained at 10 °C. In contrast, the addition of four equivalents of $P(p\text{-tolyl})_3$ to **1** in acetonitrile resulted in the formation of a precipitate of $[CpFe(CO)(\mu\text{-}CN)_2Cu\{P(p\text{-tolyl})_3\}_2]_2$ (**6**), which was stable when redissolved in either THF or dichloromethane. The conversion of complex **6** to the bimetallic complex $[CpFe\{P(p\text{-tolyl})_3\}(CN)(\mu\text{-}CN)Cu\{P(p\text{-tolyl})_3\}]_2$, in the presence of added equivalents of $P(p\text{-tolyl})_3$ in dichloromethane (ν_{CN} = 2086 sh, 2073 s cm^{-1}) proceeded more rapidly (only four days) than the corresponding process involving **3** and PCy_3. In addition the reaction of two or four equivalents of the series of phosphanes PMe_nPh_{3-n} (n = 1, 2, or 3) with complex **1** in dichloromethane have similarly provided the mono- and bisphosphane-substituted copper(I) derivatives **7**, **9**, **11**, and **8**, **10**, **12**, respectively. As is evident from the vibrational data in Table 1, the basicity of the phosphane ligand, which varies significantly from PMe_3 to PPh_2Me, has a negligible effect on the ν_{CN} and ν_{CO} values observed. Complexes **8**, **10**, and **12** were found to react more rapidly with added equivalents of the corresponding phosphane ligand to provide the bimetallic complex than previously observed for other complexes. For example, complex **12** was quantitatively converted in the presence of PMe_3 into $[CpFe(PMe_3)(CN)(\mu\text{-}CN)Cu(PMe_3)_2]$ in two days. When eight equivalents of PMe_nPh_{3-n} (n = 1, 2, or 3) were added directly to complex **1** in dichloromethane, the infrared spectra of the products were consistent with complete disruption of the parallelogram structures with concomitant formation of the $[Cu(PMe_nPh_{3-n})_4]$-$[CpFe(CO)(CN)_2]$ salts.

In studies designed to examine the nature of the complex formed when the monodentate tricyclohexylphosphane is replaced by its bidentate analogs $Cy_2P\text{-}(CH_2)_n\text{-}PCy_2$, we synthesized the derivatives where n varies from 1 to 4 in an identical manner. Infrared spectroscopic data in the ν_{CO} and ν_{CN} regions for the derivatives of dcpm [bis(dicyclohexylphosphanyl)methane] (**13**), dcpe [1,2-bis(dicyclohexylphosphanyl)ethane] (**14**), and dcpp [bis(dicyclohexylphosphanyl)propane] (**15**) are quite similar (Table 1). Furthermore, these derivatives were shown by elemental analysis to be stoichiometrically of the same composition. The most distinguishing spectral feature noted between complex **13** and complexes **14** and **15** is the magnitude of the downfield shift of the ^{31}P NMR resonance of the bisphosphane ligand upon complexation to copper(I): whereas the ^{31}P NMR shift is significantly different from that of the free phosphane in complex **13** (by 16 ppm), in complexes **14** and **15** the chemical shift difference is only 0.9−1.2 ppm (see Table 2).

X-ray Crystal Structures

X-ray quality crystals of **2** were obtained upon the slow diffusion of acetonitrile into a dichloromethane solution of the complex over several days at 10 °C. Under similar conditions, yellow or yellow-orange crystals of complexes **3**, **6**, **12**, and **15** were obtained from THF/hexane, and orange crystals of **4**, **13**, and **14** from dichloromethane/diethyl

Table 2. ^{31}P NMR spectroscopic data

Compound[a]	δ, ppm
PCy_3	10.86
$[CpFe(CO)(\mu\text{-}CN)_2Cu(PCy_3)]_2$ (**2**)	15.16
$[CpFe(CO)(\mu\text{-}CN)_2Cu(PCy_3)_2]_2$ (**3**)	11.74
$[CpFe(PCy_3)(CN)(\mu\text{-}CN)_2Cu(PCy_3)_2]$ (**4**)	80.16, 12.00
$PMePh_2$	−26.65
$[CpFe(CO)(\mu\text{-}CN)_2Cu(PMePh_2)]_2$ (**7**)	−22.08
$[CpFe(CO)(\mu\text{-}CN)_2Cu(PMePh_2)_2]_2$ (**10**)	−20.06
PMe_2Ph	−45.01
$[CpFe(CO)(\mu\text{-}CN)_2Cu(PMe_2Ph)]_2$ (**8**)	−35.48
$[CpFe(CO)(\mu\text{-}CN)_2Cu(PMe_2Ph)_2]_2$ (**11**)	−32.95
PMe_3	−60.96
$[CpFe(CO)(\mu\text{-}CN)_2Cu(PMe_3)]_2$ (**9**)	−47.48
$[CpFe(CO)(\mu\text{-}CN)_2Cu(PMe_3)_2]_2$ (**12**)	−44.79
dcpm	−9.93
$[CpFe(CO)(CN)(\mu\text{-}CN)Cu(dcpm)]_2$ (**13**)	6.20
dcpe	2.25
$[CpFe(CO)(\mu\text{-}CN)_2Cu(dcpe)]_2$ (**14**)	3.10
dcpp	−5.55
$[CpFe(CO)(\mu\text{-}CN)_2Cu(dcpp)]_2$ (**15**)	−6.71
dcpb	−4.30
$[CpFe(CO)(\mu\text{-}CN)_2Cu(dcpb)]_2$ (**16**)	−0.82

[a] Spectra determined in dichloromethane at ambient temperature.

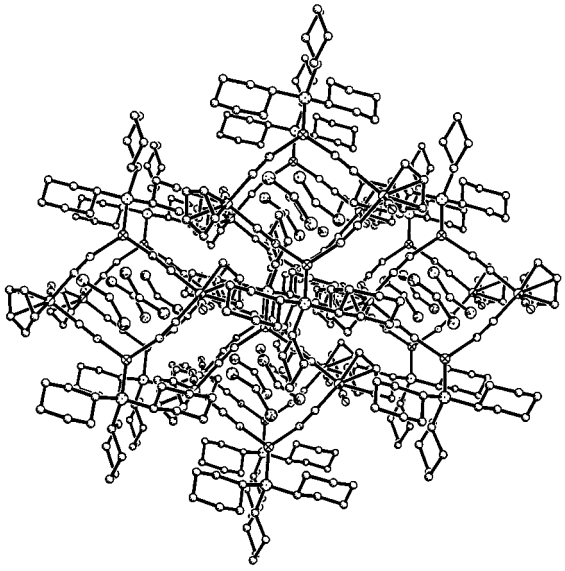

Figure 3. Crystal packing diagram of $[CpFe(CO)(\mu\text{-}CN)_2Cu(PCy_3)]_2$ (**2**)

ether. The solid-state structures of **2**, **3**, **4**, **6**, and **12**−**15** were determined by X-ray crystallographic analysis. Selected bond lengths and angles of **2**, **3**, **4**, **6**, **12**−**15** are listed in Table 3. Figure 3 presents a crystal packing diagram of complex **2**, and Figure 4 shows a thermal ellipsoid drawing of complex **3**. Complexes **2** and **3** possess a diamond-shaped motif composed of two $\eta^5\text{-}C_5H_5Fe(CO)$ fragments, two Cu^I centers, and four bridging CN groups. Due to the addition of phosphane ligands, the coordination geometry about the copper(I) centers of **2** and **3** are trigonal planar and tetrahedral, respectively. As anticipated, upon increasing the coordination number of the copper centers from three to four, i.e., proceeding from complex **2** to **3**, the average Cu−P and Cu−N bond lengths are lengthened by about 0.1 Å. As seen in Figure 4, the diamond-shaped core of complex **3** was found to be partially blocked by the cyclohexyl groups from phosphane ligands. This steric hindrance is not observed in complex **2** or in the chelated bisphosphane derivatives (vide infra). Figure 3 shows the packing diagrams for complex **2**, where solvent molecules (CH_2Cl_2) lie between the overlapping diamonds that form channels within the solids. Complex **2** is the only structurally characterized of these species that has a trigonal Cu^I center. Presumably due to the sterically encumbering PCy_3 ligand, which has a cone angle of 179°,[32] complex **2** is stabilized by filling up the coordination space of the copper centers with PCy_3. We were not able to crystallize other derivatives from solution. The insert in Figure 4 illustrates another interesting feature of the solid-state structure of **3**: the disorder of the $\eta^5\text{-}C_5H_5Fe$ fragments. This type of disorder is also found in the solid-state structure of complex **6**. This is illustrated in Figure 5, which shows that complex **6** has a structure similar to complex **3**; the ball-stick drawing of the $\eta^5\text{-}C_5H_5Fe$ disorder of complex **6** is provided as the insert of Figure 5.

Table 3. Selected bond lengths (Å) and bond angles (deg) for complexes **2**−**4**, **6** and **12**−**15**

	2	**3**	**4**	**6**	**12**	**13**	**14**	**15**
Cu−N(1)	1.957(3)	2.036(3)	1.943(9)	2.028(3)	2.032(4)	1.994(3)	1.974(5)	2.004(3)
Cu−N(2)	1.953(4)	2.020(4)	−	2.008(3)	2.010(4)		1.977(5)	1.992(3)
Cu−P(1)	2.206(2)	2.2958(10)	2.233(3)	2.2814(9)	2.2454(16)	2.2473(11)	2.2462(17)	2.2542(9)
Cu−P(2)	−	2.2622(10)	2.236(3)	2.2474(9)	2.2369(15)	2.2626(11)	2.2478(16)	2.2494(9)
Fe−C(1)	1.886(4)	1.875(5)	1.854(10)	1.923(5)	1.898(5)	1.880(4)	1.890(6)	1.898(3)
Fe−C(2)	1.897(4)	1.882(5)	1.870(13)	1.888(5)	1.901(5)	1.900(5)	1.891(6)	1.900(3)
Fe−C(3)	1.750(4)	1.737(12)	−	1.801(6)	1.731(6)	1.788(5)	1.755(6)	1.749(3)
$Fe-C_{Cp}$ (av.)	2.101	2.008	2.092	2.056	2.091	2.075	2.096	2.099
P(1)−Cu−P(2)	−	127.75(4)	139.54(11)	121.21(3)	118.71(6)	144.26(4)	92.49(6)	104.67(3)
N(1)−Cu−N(2)	109.33(13)	100.58(14)	−	106.78(11)	103.04(16)		103.93(19)	101.98(11)
Cu−N−C (av.)	160.4	166.7	166.5(9)	162.9	174.7	158.3(3)	178.9(5)	172.1(3)
Fe−C−N (av.)	175.5	178.4	172.9(10)	171.1	176.9	175.4(4)	176.9(5)	179.1(3)

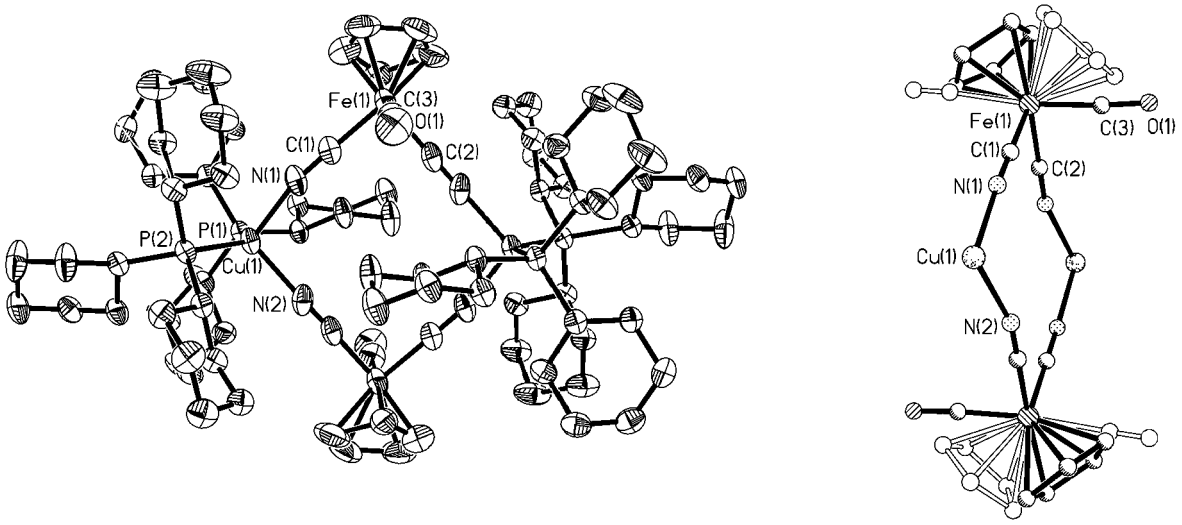

Figure 4. Thermal ellipsoid representation of $[CpFe(CO)(\mu\text{-}CN)_2Cu(PCy_3)_2]_2$ (**3**)

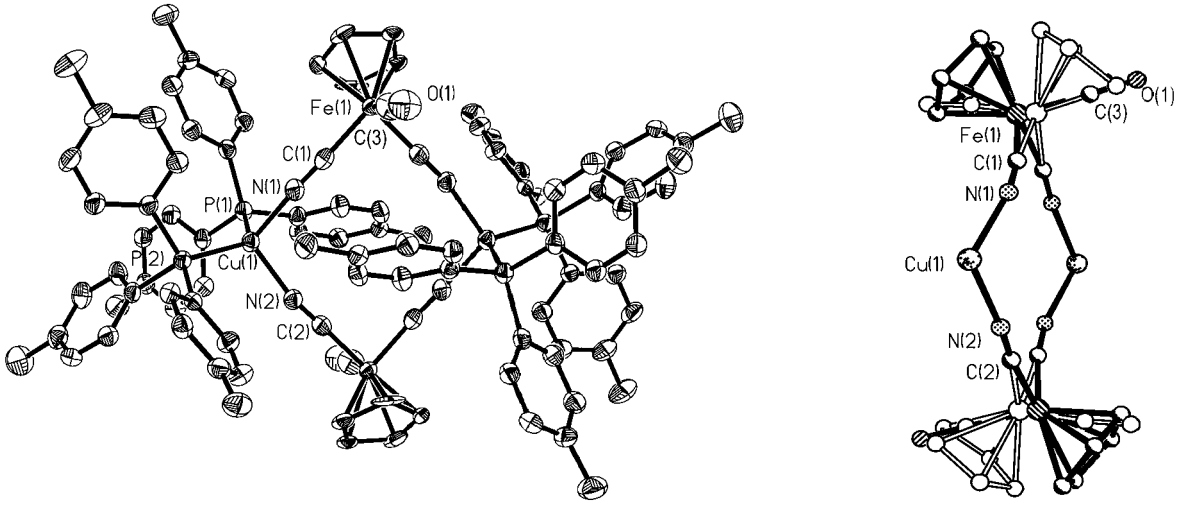

Figure 5. Thermal ellipsoid representation of $[CpFe(CO)(\mu\text{-}CN)_2Cu(P\text{-}p\text{-}totyl_3)_2]_2$ (**6**)

As previously mentioned, the prolonged exposure of complex **3** to PCy_3 in CH_2Cl_2 affords the bimetallic complex **4**, which does not contain a CO ligand bound to iron. The thermal ellipsoid representation of complex **4** is depicted in Figure 6. A tricyclohexylphosphane, a terminal CN ligand, and the bridging CN group occupy the remaining coordination sites of the CpFe moiety. The coordination geometry about the Cu^I center is trigonal, and the copper's coordination sphere is completed by the bridging CN group and two PCy_3 ligands. Apparently, complex **4** is synthesized by the substitution of CO with PCy_3 on the iron centers of **3** and the cleavage of one Cu^I-N bond on each copper center of complex **3**. The average Cu−P bond length in complex **4** (2.235 Å) is slightly shorter than those found in complex **3** (2.279 Å). Similarly, the Cu−N bond length of 1.943(9) Å is shorter than the average Cu−N bond length in **3** (2.028 Å). These bond length trends are the same as those observed in proceeding from **2** to **3**, that is, when the coordination number of copper increases from three to four. By comparing the two trigonal Cu^I centers of complexes **2** and **4**, the average Cu−P bond length in **4** (2.235 Å) is slightly longer than that in **2** [2.206(2) Å], whereas, the Cu−N bond length in **4** [1.943(9) Å] is shorter than that in **2** (1.955 Å on average). As expected, the P(I)−Cu−P(2) bond angle in complex **4** [139.54(11)°] is much larger than that found in **3** [127.75(4)°]. The bonding mode of Fe−C≡N−Cu in complex **4** is nonlinear, with Fe−C(1)−N(1) and C(1)−N(1)−Cu bond angles of 172.9(10) and 166.5(9)°, respectively.

Figure 7 shows a thermal ellipsoid drawing of $[CpFe(CO)(\mu\text{-}CN)_2Cu(PMe_3)_2]_2$ (**12**), where the basic metal cyanide core structure is similar to those seen in the other bis-bimetallic derivatives. However, in this instance the Cp and carbonyl ligands were not disordered about the $[Fe(CN)_2Cu]_2$ plane.

Furthermore, unlike the bis tricyclohexylphosphane and $P(p\text{-tolyl})_3$ analogs, the sterically less demanding PMe_3 ligands do not block the entrance to the diamond-shaped core. Instead, solvent molecules are able to occupy the channels created by the overlapping diamonds as in com-

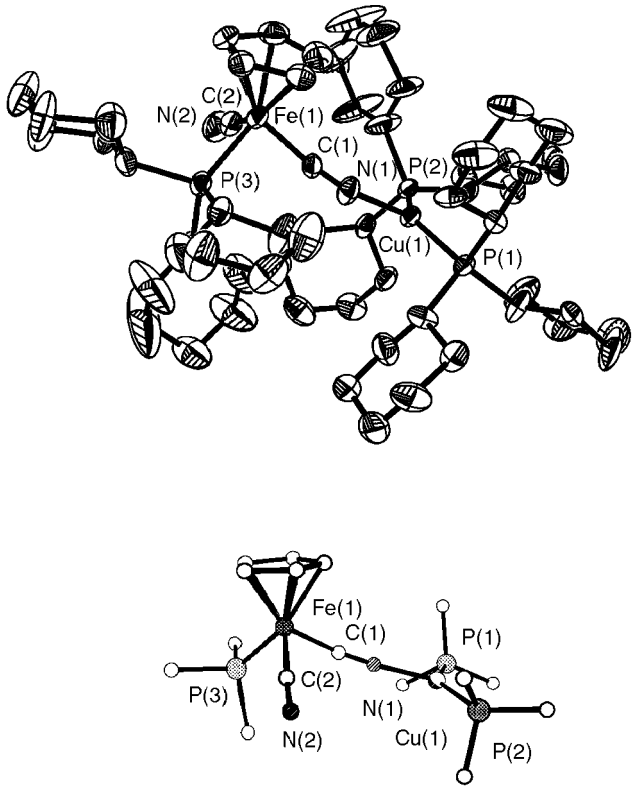

Figure 6. Thermal ellipsoid representation of $CpFe(PCy_3)(CN)(\mu\text{-}CN)Cu(PCy_3)_2$ (**4**)

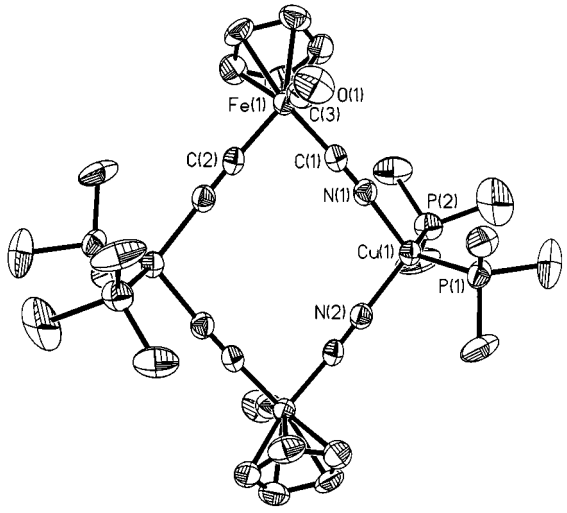

Figure 7. Thermal ellipsoid representation of $[CpFe(CO)(\mu\text{-}CN)_2Cu(PMe_3)_2]_2$ (**12**)

plex **2**. It is noteworthy that in this complex the C≡N−Cu bond angles are close to being linear, with an average bond angle of 174.7°. The corresponding average C≡N−Cu bond angles in the other crystallographically determined derivatives (complexes **2**, **3**, and **6**) cover a range of 160.4−166.7°. Although complexes **3**, **6**, and **12** have similar structures, the P−Cu−P angles and Cu−P bond lengths respond to the steric requirements of the phosphane ligands, that is, the P−Cu−P angles become more obtuse and the Cu−P bond lengths become longer with increasing phosphane cone angles (see Table 4).

A thermal ellipsoid representation of complex **13** is shown in Figure 8, and a list of selected bond lengths and angles is provided in Table 3. Unlike the bis(tricyclohexylphosphane) derivative, complex **13** consists of two Cu^I centers, each in a distorted trigonal environment, separated by 2.844 Å and bridged by the two dcpm ligands. The third ligand completing each copper center's coordination sphere is a nitrogen atom of a bridging CN group from the $CpFe(CO)(CN)_2^-$ anion. The insert in Figure 8 illustrates the distorted T-shape about the copper centers, where the P(1)−Cu(1)−P(2) angle is 144.26(4)°. Hence, like the CO ligand, one cyanide ligand of the $CpFe(CO)(CN)_2^-$ units is terminal.

As seen in Figure 8, the two $CpFe(CO)(CN)_2^-$ moieties are on opposite sides of the eight-membered metallacycle afforded by the two copper(I) atoms and the two bisphosphane ligands. The Cu−P bond lengths in complex **13** [2.2473(11) and 2.2626(11) Å] are slightly shorter than those found in the diamond-shaped bis(tricyclohexylphosphane) derivative (2.28 Å on average), where the geometry about the copper is tetrahedral with two bridging CN ligands. Similarly, the Cu−N bond length of 1.994(3) Å is shorter than the average Cu−N bond length in the bis-PCy_3 analog. These observations are to be expected in proceeding from three- to four-coordinate copper, and are also observed in the mono- and bis-tricyclohexylphosphane complexes. Interestingly, the C−N−Cu bond angle in **13** [158.3(3)°] is more acute than that found in the geometrically constrained diamond-shaped derivatives (vide infra).

Again, in an effort to conclusively define the structures of complexes **14** and **15** we have resorted to X-ray crystallography. This is of particular importance since the spectroscopic data for complexes **13**−**15** are so similar. Thermal ellipsoid drawings of complexes **14** and **15** are found in Figures 9 and 10, respectively, and lists of selected bond lengths and angles are provided in Table 3.

Table 4. Cone angles, P−Cu−P bond angles, and Cu−P bond lengths of **3**, **6**, and **12**

Compound	Cone angle (deg)	P−Cu−P (deg)	Cu−P (Å)
$[CpFe(CO)(\mu\text{-}CN)_2Cu(PCy_3)_2]_2$ (**3**)	179	127.75	2.264
$[CpFe(CO)(\mu\text{-}CN)_2Cu\{(P\text{-}p\text{-}tolyl)_3\}_2]_2$ (**6**)	145	121.21	2.279
$[CpFe(CO)(\mu\text{-}CN)_2Cu(PMe_3)_2]_2$ (**12**)	118	118.71	2.241

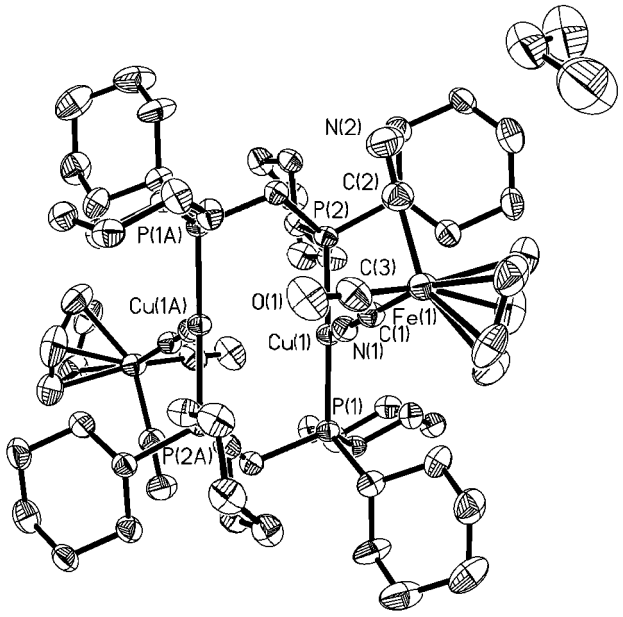

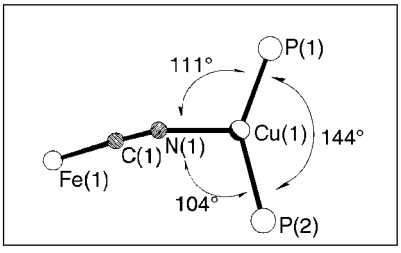

Figure 8. Thermal ellipsoid representation of complex **13**; the insert illustrates the coordination sphere about the copper(I) center

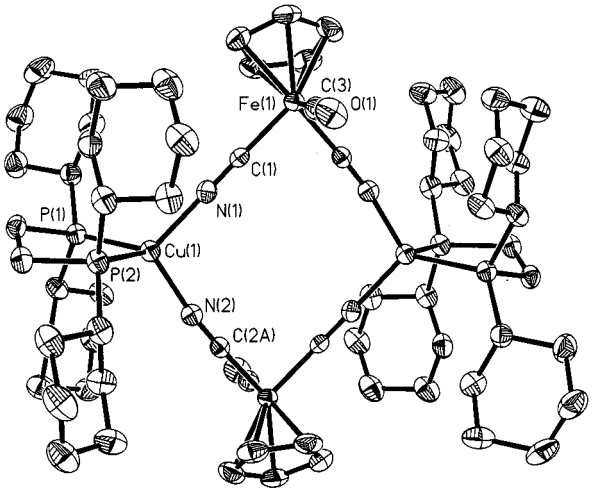

Figure 9.Thermal ellipsoid representation of complex **14**

Complex **14** crystallized with two molecules each of CH_2Cl_2 and CH_3CN, whereas complex **15** crystallized with five molecules of THF. Both derivatives possess the diamond-shaped structure previously observed in the analogous complexes containing monodentate tricyclohexylphosphane ligands. The diamond or parallelogram is formed by two iron(II) and two copper(I) atoms linked by four bridging cyanide ligands, where the carbon end of the CN group is bound to iron and the nitrogen end to copper. The coppers' coordination spheres are completed by a chelating bisphosphane ligand. Hence, upon changing the number of methylene groups between the two PCy_2 donors from one to two or three, the bisphosphanes switch from bridging to chelating with regard to their binding to the copper(I) centers. The two iron-bound terminal CO ligands lie on opposite sites of the plane defined by the four metal atoms.

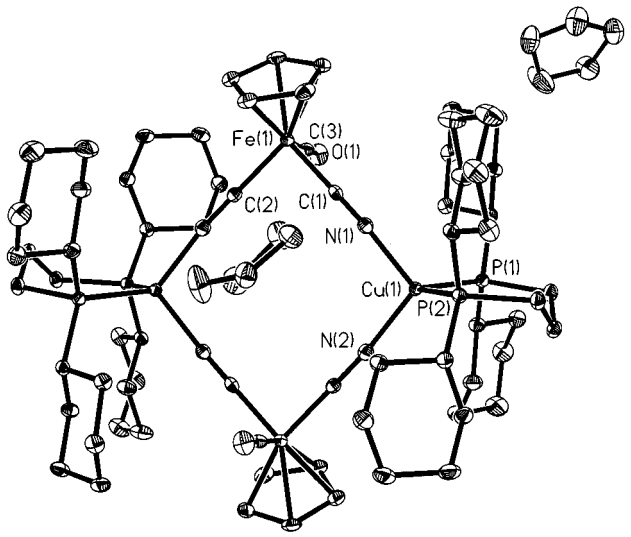

Figure 10. Thermal ellipsoid representation of complex **15**

The average Cu−N and Cu−P bond lengths were found to be 1.975(5) and 2.247(2) Å in **14**, and 1.998(3) and 2.252(1) Å in **15**, respectively. These bond parameters are quite similar to those found in complex **13**. The P−Cu−P angle in **14** at 92.49(6)° is, as expected, more acute than that seen in complex **15** [104.69(4)°] due to the change in going from a five-membered chelate ring to a six-membered chelate ring. On the other hand, the N−Cu−N angles are quite similar in the two diamond-shaped complexes at 103.93(19) and 101.93(12)°, in **14** and **15** respectively. Similarly, the C−Fe−C angles in the two parallelograms differ only slightly, 87.0(2) in **14** and 87.99(14)° in **15**. In contrast to complex **13**, where the Cu−N−C−Fe linkage is highly nonlinear, in complexes **14** and **15** which contain C−N−Cu average angles of 175.8(5) and 172.0(3)° and N−C−Fe average angles of 177.3(5) and 179.2(3)°, this unit is fairly linear.

The geometric dimensions of the Fe_2Cu_2 diamond-shaped core in complexes **14** and **15** are summarized in Figure 11. The internal area of the diamond is approximately 25 $Å^2$. As is seen in the space-filling model of **15** (Figure 12) access to the internal void space, which can accommodate a sphere with a radius up to approximately 1.04 Å, is ready available in the case of the chelated cyclohexylphosphane ligands. This is *not* the case in the analogous bis PCy_3 derivative where the cyclohexyl rings partially block the opening. Figure 13 displays a packing diagram for complex **14**, where

between the layers of overlapping diamonds, which form channels in the solids, there are solvate molecules of CH_3CN.

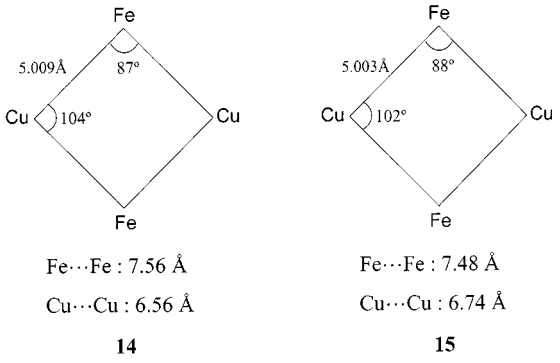

Figure 11. Metric parameters of the $Fe_2Cu_2(CN)_4$ cores of complexes **14** and **15**

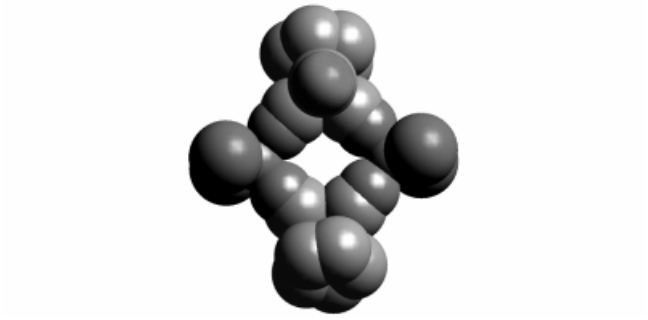

Figure 12. Space-filling model of complex **15**

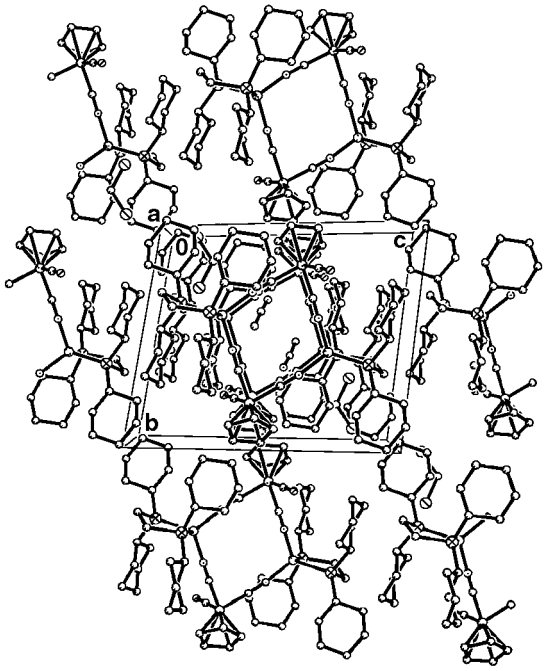

Figure 13. Packing diagram for complex **14**, indicating solvent molecules between the layers of the stacked diamond-shaped complexes

Since we have observed $[CpFe(CO)(\mu\text{-}CN)_2CuPCy_3]_2$, where the copper(I) center is trigonal, to be quite stable, it was of interest to examine the effect of extending the number of methylene units in the $Cy_2P(CH_2)_nPCy_2$ ligand to four. In this instance the bisphosphane ligand may have a greater propensity for affording linked chains of diamond-shaped moieties as opposed to chelating to a single copper(I) center. Hence, the synthesis of the derivative with $Cy_2P(CH_2)_4PCy_3$ (dcpb) (**16**) was performed in a completely analogous manner to that employed for complexes **14** and **15**. Unfortunately, we have yet to obtain X-ray quality crystals of **16**, and therefore have not been able to definitively identify its structure. However, based on the close spectral resemblance of complex **16** to complexes **14** and **15** (see Table 1), coupled with its ready solubility, we suggest it to be the seven-membered chelate bisphosphane derivative.

Solution ^{31}P NMR Spectroscopy

Table 2 lists the ^{31}P NMR spectra in CH_2Cl_2 of the heterobimetallic complexes synthesized and structurally characterized in this report. As seen in Table 2 and Figures 14A and 14B, the ^{31}P NMR resonances for complexes **2** and **3**, the mono- and bis-tricyclohexylphosphane derivatives of $[CpFe(CO)(\mu\text{-}CN)_2Cu]_2$, at ambient temperature are shifted slightly downfield from the free ligand at $\delta = 15.16$ and 11.74, respectively, and are somewhat broadened with frequency width half-height (fwhh) values of 106 and 65 Hz, respectively. This is presumably due to line broadening by

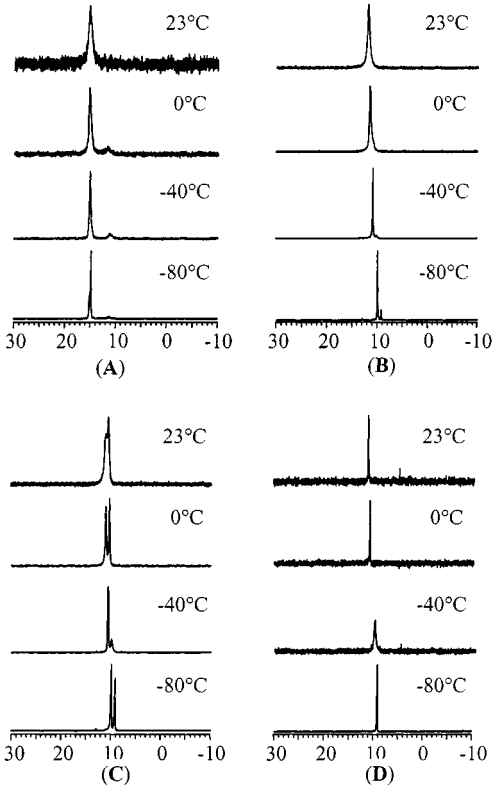

Figure 14. Variable temperature ^{31}P NMR spectra of $[CpFe(CO)(\mu\text{-}CN)_2Cu(PCy_3)]_2$ (**A**), $[CpFe(CO)(\mu\text{-}CN)_2Cu(PCy_3)_2]_2$ (**B**), $[CpFe(CO)(\mu\text{-}CN)_2Cu(PCy_3)_2]_2 + PCy_3$ (**C**), and PCy_3 (**D**)

the quadrupolar nuclei ^{63}Cu and ^{65}Cu. By way of contrast, the free PCy_3 ligand has a resonance at $\delta = 10.86$ with a fwhh of only 11 Hz at ambient temperature. Nevertheless, there is a temperature dependence of the free PCy_3 ligand with broadening being noted around −40 °C; this can be attributed to the conformation exchange of the chair and boat forms of the cyclohexyl rings (see Figure 14D).

Upon the addition of two equivalents of PCy_3 to complex **3** in dichloromethane the ^{31}P NMR spectrum exhibits resonances for both complex **3** and free PCy_3. These ^{31}P NMR signals display the same temperature behavior noted for the individually determined spectra, i.e., the sum of the spectra in Figure 14B and 14D afford that seen in Figure 14C. These ^{31}P NMR spectral results are indicative of *slow phosphane exchange* between complex **3** and PCy_3 ($<<100$ sec^{-1}). Furthermore, the infrared spectra of complexes **2** and **3** clearly indicate that there is only one principal species in pure solutions of these two derivatives, as can be seen from the overlapping spectra in the ν(CN) region in Figure 15. As previously indicated prolonged standing of the reaction solution containing complex **3** and PCy_3 affords complex **4**, where the phosphorous resonance for PCy_3 bound to iron is observed at $\delta = 80.2$.

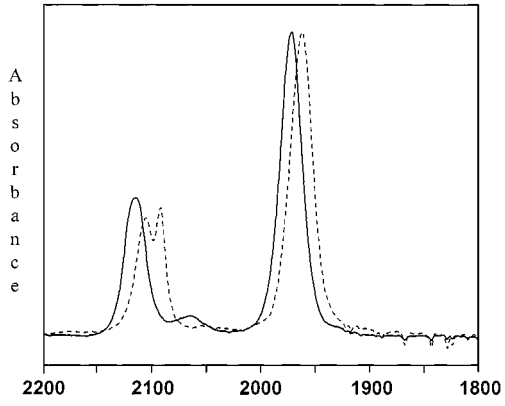

Figure 15. Superimposition of the infrared spectra of complexes **2** (——) and **3** (- - - -)

There is a trend noted in the ^{31}P NMR resonance of the methyl(phenyl)phosphane derivatives. That is, the more basic phosphane derivative shows an increased downfield shift in the complex compared to that of the free phosphane ligand (Table 2). These differences in chemical shift range from the most basic PMe_3 derivative (**9**; $\delta = 13.48$) to the least basic PPh_2Me derivative (**7**; $\delta = 4.04$). In addition, the ^{31}P NMR resonances of the derivatives containing two phosphanes per copper center all fall downfield from their one-phosphane-bound counterparts by about 2 ppm.

Concluding Remarks

Encompassed in this report are contributions to the growing body of work on the synthesis and structural characterization of metallacyclic polygons,[1] in particular those containing cyanide bridges.[2−27] Among the iron(II)/copper(I) cyanide-bridged bimetallic complexes we have synthesized, **13** is the only complex composed of an eight-membered metallacycle with a short $Cu^{I}\cdots Cu^{I}$ distance in the solid-state due to dcpm bridging the two copper(I) centers. As the number of methylene groups between the PCy_2 donors of the bisphosphane ligand is increased, the bisphosphane changes its bonding mode from bridging to chelating. Hence, the X-ray structures of complexes **14** and **15**, which contain the bisphosphane ligands dcpe and dcpp, respectively, show an Fe_2Cu_2 diamond-shaped core as seen in the monodentate phosphane derivatives **2**, **3**, **6**, and **12**, e.g., $[CpFe(CO)(\mu\text{-}CN)_2(PCy_3)_2]_2$, where the copper(I) centers are four coordinate. The diamond-shaped core can readily accommodate a sphere with a radius of up to 1.04 Å. In contrast to the bis(tricyclohexylphosphane) derivative, the cores of **12**, **14** and **15** are not blocked by cyclohexyl groups. Therefore, solvent molecules are able to occupy the channels created by the overlapping diamonds in the solids. In general the Cu−N−C−Fe linkage is nonlinear, with the Cu−N−C and Fe−C−N angles covering a range of 158.3 to 178.9° and 171.1 to 179.1°, respectively.

Experimental Section

Methods and Materials: All manipulations were performed under argon using standard Schlenk and glovebox techniques. Acetonitrile was distilled once from CaH_2 and once from P_2O_5 and then freshly distilled from CaH_2 immediately before use. Dichloromethane was dried and distilled over P_2O_5. Hexane, diethyl ether, and THF were dried in sodium benzophenone stills prior to use. The following reagents were used as received without further purification: Cyclopentadienylirondicarbonyl dimer, tetrafluoroboric acid, dimethylphenylphosphane (Aldrich); bromine (EM Science); potassium cyanide, cuprous oxide, triphenylphosphane (Fisher Scientific); tricyclohexylphosphane, trimethylphosphane, methyldiphenylphosphane, tri-*p*-tolylphosphane (Strem), bis(dicyclohexylphosphanyl)methane, dcpm (Strem), 1,2-bis(dicyclohexylphosphanyl)ethane, dcpe (Strem), 1,3-bis(dicyclohexylphosphanyl)-propane, dcpp (Aldrich), 1,4-bis(dicyclohexylphosphanyl)butane, dcpb (Aldrich). $[Cu(CH_3CN)_4][BF_4]$[33] and $K[CpFe(CO)(CN)_2]$[34] salts were prepared according to published literature procedures.

Infrared spectra were recorded on a Mattson 6021 FTIR using a 0.1 mm CaF_2-sealed cell for solutions and KBr pellets for solid samples. All ^{31}P NMR spectra were recorded on a Varian Unity Plus 300 MHz spectrometer (121.4 MHz ^{31}P) using non-deuterated dichloromethane as solvent. The magnetic field was locked with deuterium oxide, and a tube with an 85% phosphoric acid solution was used as an external reference. Variable temperature ^{31}P NMR spectra were recorded every 20 °C from +20 to −80 °C using liquid N_2 as coolant. Elemental analyses were carried out by Canadian Microanalytical Service, Ltd., Canada.

Synthesis of $[CpFe(CO)(\mu\text{-}CN)_2Cu(CH_3CN)_2]_2$ (1): Acetonitrile (10 mL) was added to a mixture of $K[CpFe(CO)(CN)_2]$ (0.2 mmol, 0.048 g) and $[Cu(CH_3CN)_4][BF_4]$ (0.2 mmol, 0.0628 g) in a 50 mL Schlenk flask. After 30 min. of stirring at ambient temperature a pale gray solid of KBF_4 precipitated from the yellow reaction mixture. The KBF_4 salt was separated from the yellow solution of **1** by filtration. The acetonitrile solution of **1** was used immediately in the following syntheses.

Synthesis of $[CpFe(CO)(\mu\text{-}CN)_2Cu(PCy_3)]_2$ (2): An acetonitrile solution of **1** prepared as described above was added to a 50 mL Schlenk flask containing 0.2 mmol of tricyclohexylphosphane (0.056 g). The crude product precipitated out as a yellow solid. Upon removal of the solvent by cannula and vacuum, the remaining solid was isolated in ca. 91% yield. X-ray quality crystals of **2** were obtained upon slow diffusion of acetonitrile into a dichloromethane solution of **2** maintained at 10 °C for several days. − $[CpFe(CO)(CN)_2Cu(PCy_3)]_2 \cdot 1.5CH_2Cl_2$: calcd. C 52.79, H 6.54, N 4.60; found C 52.90, H 7.21, N 4.36.

Synthesis of $[CpFe(CO)(\mu\text{-}CN)_2Cu(PCy_3)_2]_2$ (3). Method I: Complex **3** was synthesized as described above for complex **2** employing 0.4 mmol of PCy_3 (0.112 g). A clear yellow solution of **3** was obtained in acetonitrile. Upon removal of the solvent by vacuum, a crude product of **3** was obtained as a yellow solid (yield 92%). Yellow orange crystals of **3** were obtained by slow diffusion of hexane into a THF solution of **3**. − $[CpFe(CO)(CN)_2Cu(PCy_3)]_2 \cdot 2THF$: calcd. C 64.24, H 8.87, N 3.12; found C 63.60, H 10.13, N 2.43.

Method II: Complex **3** could also be synthesized by adding two equivalents of PCy_3 to complex **2** in dichloromethane.

Synthesis of $[CpFe(PCy_3)(CN)(\mu\text{-}CN)Cu(PCy_3)_2]$ (4): A 5 mL dichloromethane solution of PCy_3 (0.2 mmol, 0.056 g) was added to a 10 mL dichloromethane solution of complex **3** (0.1 mmol, 0.165 g). An olive solution was formed along with some gray precipitate after two weeks of stirring. The gray precipitate was separated by filtration, and complex **4** was isolated by recrystallization. X-ray quality crystals of **4** were obtained by slow diffusion of diethyl ether into a dichloromethane solution of **4**.

Synthesis of $[CpFe(CO)(\mu\text{-}CN)_2Cu(P\text{-}p\text{-}Tol_3)]_2$ (5): The synthesis of complex **5** was carried out exactly as described above for complex **2** employing tri-*p*-tolylphosphane (0.2 mmol, 0.061 g). A yellow solution of **5** resulted; unfortunately, complex **5** decomposes at ambient temperature.

Synthesis of $[CpFe(CO)(\mu\text{-}CN)_2Cu(P\text{-}p\text{-}Tol_3)_2]_2$ (6): An acetonitrile solution of **1** as described above was added to a 50 mL Schlenk flask containing 0.4 mmol of tri-*p*-tolylphosphane (0.122 g). The reaction solution was stirred for 30 min., and **6** formed as a yellow precipitate. Upon removing the solvent by cannula and vacuum, the yellow solid was isolated in 90% yield. Yellow crystals of **6** were obtained upon slow diffusion of hexane into a THF solution of **6** at 10 °C for several days. − Calcd. C 68.77, H 5.42, N 3.21; found C 68.23, H 5.50, N 3.13.

Synthesis of $[CpFe(CO)(\mu\text{-}CN)_2CuL]_2$ [L = $PMePh_2$ (7), PMe_2Ph (9), PMe_3 (11)]: A 5 mL acetonitrile solution of phosphane (0.2 mmol, 0.015 g for PMe_3, 0.028 g for PMe_2Ph, and 0.040 g for $PMePh_2$) was slowly added to a yellow acetonitrile solution of **1**. A yellow-orange solution was obtained for each phosphane derivative. Upon removing the solvent by vacuum, yellow-orange solids were isolated.

Synthesis of $[CpFe(CO)(\mu\text{-}CN)_2CuL_2]_2$ [L = $PMePh_2$ (8), PMe_2Ph (10), PMe_3 (12)]: The syntheses of complexes **8**, **10**, and **12** were carried out as described above for **7**, **9**, and **11** with 0.4 mmol of phosphane (0.030 g for PMe_3, 0.056 g for PMe_2Ph, and 0.080 g for $PMePh_2$). X-ray quality crystals were obtained by slow diffusion of hexane into a THF solution of **12**.

Synthesis of $[CpFe(CO)(CN)(\mu\text{-}CN)Cu(dcpm)]_2$ (13): A 10 mL dichloromethane solution of dcpm (0.20 mmol, 0.081 g) was added to an acetonitrile solution of **1** prepared as described above. The reaction solution was stirred for 30 min. at ambient temperature, followed by removal of the mixed solvent under vacuum to afford a yellow residue in 92% yield. Yellow-orange crystals of **13** were obtained by slow diffusion of diethyl ether into a dichloromethane solution of **13** maintained at 10 °C for several days. − $C_{66}H_{102}Cu_2Fe_2N_4O_2P_4$ (1346.24): calcd. C 58.88, H 7.64, N 4.16; found C 58.10, H 8.00, N 3.98.

Synthesis of $[CpFe(CO)(\mu\text{-}CN)_2Cu(dcpe)]_2$ (14): The synthesis of this derivative was carried out exactly as described above for complex **13** employing 0.20 mmol (0.084 g) of dcpe. The yellow-orange product was recovered upon removing the mixed solvent under vacuum. Orange crystals of **14** were obtained from CH_2Cl_2/diethyl ether maintained at 10 °C over several days. − $C_{68}H_{106}Cu_2Fe_2N_4O_2P_4 \cdot 2CH_2Cl_2$: calcd. C 54.45, H 7.18, N 3.63; found C 55.29, H 7.97, N 3.97.

Synthesis of $[CpFe(CO)(\mu\text{-}CN)_2Cu(dcpp)]_2$ (15): Alternatively, the reaction between $K[CpFe(CO)(CN)_2]$ (0.20 mmol, 0.048 g) and $[Cu(CH_3CN)_3][BF_4]$ (0.20 mmol, 0.063 g) was carried out directly in dichloromethane for 30 min. followed by filtration to remove the KBF_4 salt. Subsequently, dcpp (0.20 mmol, 0.087 g) in 10 mL of dichloromethane was added dropwise to the yellow filtrate and the solution stirred at room temperature for 30 min. to yield a yellow solution. Upon removal of the solvent under vacuum, the yellow solid was redissolved in THF for recrystallization. Yellow crystals of **15** were obtained upon slow diffusion of hexanes into a THF solution of **15** maintained at 10 °C for several days.

X-ray Crystallography: A yellow or yellow-orange crystal of **2**, **3**, or **4** was mounted on a glass fiber with epoxy cement and placed in a cold nitrogen stream at 193 K. X-ray crystallographic data of **2**, **3**, and **4** were obtained on a Siemens R3m/V single-crystal X-ray diffractometer operating at 55 kV and 30 mA, Mo-K_α (λ = 0.71073 Å) radiation equipped with a Siemens LT-2 cryostat. Diffractometer control software P3VAX 3.42 was supplied by Siemens Analytical Instruments, Inc. Crystals of **6** and **12**−**15** were coated by mineral oil and mounted on a glass fiber with apiezon grease at room temperature. The mounted crystal was then placed in a cold nitrogen stream (Oxford) maintained at 110 K on a Bruker SMART 1000 three-circle goniometer. X-ray data of **6** and **12**−**15** were obtained on a Bruker CCD diffractometer and covered more than a hemisphere of reciprocal space by a combination of three sets of exposures.

Crystal data and details of data collection for complexes **2**, **3**, **4, 6,** and **12**−**15** are provided in Table 5. The structures were solved by direct methods. Full-matrix least-squares anisotropic refinement for all non-hydrogen atoms yielded $R(F)$ and $wR(F^2)$ values as indicated in Table 5 at convergence. Hydrogen atoms were placed in idealized positions with isotropic thermal parameters fixed 1.2- or 1.5-times the value of the attached atom. Neutral atom scattering factors and anomalous scattering factors were taken from the International Tables for X-ray Crystallography Vol. C.

For complexes 2, 3, 4, 6, and 12−15, program(s) used to solve the structure: SHELXS-86 (Sheldrick[35]); program(s) used to refine the structure: SHELXL-97 (Sheldrick[36]); program(s) used for molecular graphics: SHELXTL version 5.0 (Bruker[35]); software used to prepare material for publication: SHELXTL version 5.0 (Bruker[37]).

Crystallographic data (excluding structure factors) for the structures reported in this paper have been deposited with the Cambridge Crystallographic Data Centre as supplementary publication nos. CCDC-118334 (**2**), -168366 (**3**), -168367 (**4**), -168368 (**6**),

Table 5. X-ray crystallographic data for complexes **2**−**4**, **6**, and **12**−**15**

	2	**3**	**4**	**6**	**12**	**13**	**14**	**15**
Formula	$C_{52}H_{76}Cu_2Fe_2N_4O_2P_2 \cdot 2CH_2Cl_2$	$C_{88}H_{142}Cu_2Fe_2N_4O_2P_4 \cdot 2C_4H_8O$	$C_{61}H_{104}CuFeN_2P_3 \cdot 2CH_2Cl_2$	$C_{100}H_{94}Cu_2Fe_2N_4O_2P_4 \cdot 2C_4H_8O$	$C_{28}H_{46}Cu_2Fe_2N_4O_2P_4 \cdot 2CH_2Cl_2$	$C_{33}H_{51}CuFeN_2OP_2 \cdot CH_2Cl_2$	$C_{68}H_{106}Cu_2Fe_2N_4O_2P_4 \cdot 2CH_2Cl_2 \cdot 2CH_3CN$	$C_{55}H_{55}CuFeN_2OP_2 \cdot 2.5C_4H_8O$
Formula wt. (g/mol)	1259.74	1794.92	1247.61	1890.66	1003.20	758.01	1626.19	881.40
Crystal system	Triclinic	Triclinic	Monoclinic	Triclinic	Monoclinic	Triclinic	Triclinic	Triclinic
Space group	$P\bar{1}$	$P\bar{1}$	$P2_1/c$	$P\bar{1}$	$P2_1/n$	Pi	Pi	Pi
a (Å)	9.615(8)	13.3707(9)	12.815(6)	11.6307(11)	10.799(4)	11.6437(8)	12.7117(11)	13.363(2)
b (Å)	10.700(11)	13.8757(18)	18.698(5)	13.2303(12)	11.477(4)	11.7162(8)	12.7254(11)	13.568(2)
c (Å)	14.918(11)	15.1154(16)	27.766(6)	16.3741(16)	18.081(6)	15.0748(11)	14.6351(13)	15.616(3)
α (deg)	84.06(7)°	67.049(9)	−	92.829(2)	−	104.4820(10)	89.812(2)	65.369(3)
β (deg)	82.86(6)°	69.703(7)	92.35(3)	105.674(2)	97.943(7)	107.1720(10)	69.976(2)	69.598(3)
γ (deg)	75.56(8)°	80.748(9)	−	99.244(2)	−	102.6400(10)	67.664(2)	64.211(3)
Volume (Å)^3	1471(2)	2411.2(4)	6648(4)	2383.0(4)	2219.4(13)	1804.7(2)	2035.4(3)	2268.4(7)
Z	1	1	4	1	2	2	1	2
d_{calcd} (g/cm^3)	1.422	1.236	1.247	1.317	1.501	1.395	1.327	1.290
Temperature (K)	193	193	193	110	110	110	110	110
Wavelength (Å)	0.71073	0.71073	0.71073	0.71073	0.71073	0.71073	0.71073	0.71073
Abs. coeff. mm^{-1}	1.475	0.846	0.809	0.860	1.866	1.257	1.120	0.900
Goodness of fit on F^2	1.101	0.983	0.850	1.038	0.625	1.066	0.958	0.926
R [a]	3.92	7.13	10.00	6.72	6.54	7.61	8.85	3.62
R_w [b]	5.02	15.99	19.45	8.42	10.63	21.47	22.19	8.15

[a] $R = \Sigma||F_o| - |F_c||/\Sigma F_o$. − [b] $R_w = \{[\Sigma w(F_o^2 - F_c^2)^2]/[\Sigma w(F_o^2)^2]\}^{1/2}$.

-168362 (**12**), -168363 (**13**), -168364 (**14**), -168365 (**15**). Copies of the data can be obtained free of charge on application to CCDC, 12 Union Road, Cambridge CB2 1EZ, UK [Fax: (internat.) + 44-1223/336-033; E-mail: deposit@ccdc.cam.ac.uk].

Acknowledgments

Financial support from the National Science Foundation (CHE-99−10342 and CHE 98−07975 for the purchase of X-ray equipment), the Robert A. Welch Foundation, and by the Texas Advanced Research Technology Program (Grant No. 0390−1999) is greatly appreciated.

[1] [1a] S. Leininger, B. Olenyuk, P. J. Stang, *Chem. Rev.* **2000**, *100*, 853−908. − [1b] M. Fujita, *Chem. Soc. Rev.* **1998**, *27*, 417−425. − [1c] S. Bélanger, M. H. Keefe, J. L. Welch, J. T. Hupp, *Coord. Chem. Rev.* **1999**, *190*−*192*, 29−45.

[2] S. M. Contakes, K. K. Klausmeyer, T. B. Rauchfuss, *Inorg. Chem.* **2000**, *39*, 2069−2075; S. M. Contakes, K. K. Klausmeyer, R. M. Milberg, S. R. Wilson, T. B Rauchfuss, *Organometallics* **1998**, *17*, 3633−3635.

[3] D. Williams, J. Kouvetakis, M. O'Keeffe, *Inorg. Chem.* **1998**, *37*, 4617−4620.

[4] [4a] G. N. Richardson, H. Vahrenkamp, *J. Organomet. Chem.* **2000**, *593*−*594*, 44−48. − [4b] H. Vahrenkamp, A. Geiss, G. N. Richardson, *J. Chem. Soc., Dalton Trans.* **1997**, 3643−3651.

[5] J. J. Rupp, D. F. Shriver, *Inorg. Chem.* **1967**, *6*, 755−761.

[6] J. Emri, B. Györi, A. Bakos, G. Czira, *J. Organomet. Chem.* **1976**, *112*, 325−331.

[7] C. Carini, C. Pelizzi, G. Pelizzi, G. Predieri, P. Tarasconi, F. Vitali, *J. Am. Chem. Soc. Commun.* **1990**, 613−614.

[8] J. A. Smith, J.-R. Galán-Mascarós, R. Clérac, K. R. Dunbar, *Chem. Commun.* **2000**, 1077−1078; K. R. Dunbar, R. Heitz, *Prog. Inorg. Chem.* **1997**, *93*, 283−291.

[9] W. P. Fehlhammer, M. Fritz, *Chem. Rev.* **1993**, *93*, 1243−1280.

[10] M. Adam, A. K Brimah, R. D. Fischer, L. Xing-Fu, *Inorg. Chem.* **1990**, *29*, 1597.

[11] D. J. Darensbourg, J. C. Yoder, M. W. Holtcamp, K. K. Klausmeyer, J. H. Reibenspies, *Inorg. Chem.* **1996**, *35*, 4764−4769.

[12] M. Ohba, H. Okawa, *Coord. Chem. Rev.* **2000**, *198*, 313−328.

[13] N. Mondal, M. K. Saha, B. Bag, S. Mitra, V. Gramlich, J. Ribas, M. S. E. Fallah, *J. Chem. Soc., Dalton Trans.* **2000**, 1601−1604.

[14] V. P. Fedin, A. V. Virovets, I. V. Kalinina, V. N. Ikorskii, M. R. J. Elsegood, W. Clegg, *Eur. J. Inorg. Chem.* **2000**, 2341−2343.

[15] E. Colacio, J. M. Domínguez-Vera, M. Ghazi, R. Kivekäs, J. M. Moreno, A. Pajunen, *J. Chem. Soc., Dalton Trans.* **2000**, 505−509.

[16] N. G. Connelly, O. M. Hicks, G. R. Lewis, A. G. Orpen, A. J. Wood, *J. Chem. Soc., Dalton Trans.* **2000**, 1637−1643.

[17] P. Fspinet, K. Soulantica, J. P. H. Charmant, A. G. Orpen, *Chem. Commun.* **2000**, 915−916.

[18] Y. Zhao, M. Hong, W. Su, R. Cao, Z. Zhou, A. S. C. Chan, *J. Chem. Soc., Dalton Trans.* **2000**, 1685−1686.

[19] D. G. Fu, J. Chen, X. S. Tan, L. J. Jiang, S. W. Zhang, P. J. Zheng, W. X. Tang, *Inorg. Chem.* **1997**, *36*, 220−225.

[20] M. Fritz, D. Rieger, E. Bär, G. Beck, J. Fuchs, G. Holzmann, W. P. Fehlhammer, *Inorg. Chim. Acta* **1992**, *198*−*200*, 513−526.

[21] P. Schinnerling, U. Thewalt, *J. Organomet. Chem.* **1992**, *431*, 41−45.

[22] A. Christofides, N. G. Connelly, H. J. Lawson, A. C. Loyns, A. G. Orpen, M. O. Simmonds, G. H. Worth, *J. Chem. Soc., Dalton Trans.* **1991**, 1595−1601.

[23] C. Carini, C. Pelizzi, G. Pelizzi, G. Predieri, P. Tarasconi, F. Vitali, *Chem. Commun.* **1990**, 613−614.

[24] G. Lavigne, N. Lugan, J.-J. Bonnet, *Chem. Commun.* **1987**, 957−958.

[25] H. Oshio, O. Tamada, H. Onodera, T. Ito, T. Ikoma, S. Tero-Kubota, *Inorg. Chem.* **1999**, *38*, 5686−5689.

[26] [26a] S. M. Contakes, T. B. Rauchfuss, *Angew. Chem. Int. Ed.* **2000**, *39*, 1984−1986. − [26b] K. K. Klausmeyer, S. R. Wilson, T. B. Rauchfuss, *J. Am. Chem. Soc.* **1999**, *121*, 2705−2711. − [26c] K. K. Klausmeyer, T. B. Rauchfuss, S. R. Wilson, *Angew. Chem. Int. Ed.* **1998**, *37*, 1694−1696.

[27] [27a] P. A. Berseth, J. J. Sokol, M. P. Shores, J. L. Heinrich, J. R. Long, *J. Am. Chem. Soc.* **2000**, *122*, 9655−9662. − [27b] J. L. Heinrich, P. A. Berseth, J. R. Long, *Chem. Commun.* **1998**, 1231−1232. − [27c] L. G. Beauvais, M. P. Shores, J. R. Long, *J. Am. Chem. Soc.* **2000**, *122*, 2763−2772. − [27d] M. V. Ben-

nett, M. P. Shores, L. G. Beauvais, J. R. Long, *J. Am. Chem. Soc.* **2000**, *122*, 6664−6668. − [27e] M. P. Shores, L. G. Beauvais, J. R. Long, *Inorg. Chem.* **1999**, *38*, 1648−1649.
[28] [28a] A. Geiss, H. Vahrenkamp, *Inorg. Chem.* **2000**, *39*, 4029−4036 and references therein. − [28b] C. Díaz, A. Arancibia, *Inorg. Chim. Acta* **1998**, *269*, 246−252. − [28c] J. Larionova, M. Gross, M. Pilkington, H. Andres, H. Stoeckli-Evans, H. U. Güdel, S. Decurtins, *Angew. Chem. Int. Ed.* **2000**, *39*, 1605−1609.
[29] [29a] B. S. Lim, R. H. Holm, *Inorg. Chem.* **1998**, *37*, 4898−4908. − [29b] D. M. Corsi, N. N. Murthy, V. G. Young, Jr., K. D. Karlin, *Inorg. Chem.* **1999**, *38*, 848−858.
[30] D. J. Darensbourg, W.-Z. Lee, M. J. Adams, D. L. Larkins, J. H. Reibenspies, *Inorg. Chem.* **1999**, *38*, 1378−1379.
[31] [31a] B. Le-Khac, U. S. Patent 5,482,908, **1996**. − [31b] W. J. Kruper, Jr., D. J. Swart, U. S. Patent 4,500,704, **1985**.
[32] C. A. Tolman, *Chem. Rev.* **1977**, *77*, 313−348.
[33] G. J. Kubas, in *Inorg. Synth.* (Ed.: D. F. Shriver); John Wiley and Sons: New York, 1979; Vol. 19, p. 90.
[34] [34a] C. E. Coffey, *Inorg. Nucl. Chem.* **1963**, *25*, 179. − [34b] C.-H. Lai, W.-Z. Lee, M. L. Miller, J. H. Reibenspies, D. J. Darensbourg, M. Y. Darensbourg, *J. Am. Chem. Soc.* **1998**, *120*, 10103−10114.
[35] G. Sheldrick, SHELXS-86 *Program for Crystal Structure Solution*, (1986), Institut fur Anorganische Chemie der Universitat, Tammanstraße 4, 3400 Göttingen, Germany.
[36] G. Sheldrick, SHELXL-97 *Program for Crystal Structure Refinement*, (1997), Institut fur Anorganische Chemie der Universitat, Tammanstraße 4, 3400 Göttingen, Germany.
[37] Bruker, SHELXTL version 5.0, (1999), Madison, WI, USA.

Received May 3, 2001
[I01153]